

Fully quantum embedding with density functional theory for full configuration interaction quantum Monte Carlo

Hayley R. Petras,^{1,2, a)} Daniel Graham,^{3, a)} Sai Kumar Ramadugu,^{1,2} Jason D. Goodpaster,³ and James J. Shepherd^{1,2, b)}

¹⁾Department of Chemistry, University of Iowa

²⁾University of Iowa Informatics Initiative, University of Iowa

³⁾Department of Chemistry, University of Minnesota

(Dated: June 11, 2019)

In common with many high-accuracy electronic structure methods, the initiator adaptation of full configuration interaction quantum Monte Carlo (*i*-FCIQMC) has difficulty treating realistic systems with large numbers of electrons. This barrier has prevented the application of *i*-FCIQMC to questions of catalysis that, even for the simplest of models, require high-accuracy modeling of several features of the electronic structure, such as strong and dynamic correlation, and localized vs. delocalized bonding. We here present a fully-quantum embedded version of *i*-FCIQMC, which we apply to calculate the bond dissociation energy of an ionic bond (LiH) and a covalent bond (HF) physisorbed to a benzene molecule. The embedding is performed using a recently-developed Huzinaga projection operator approach, which affords good synergy with *i*-FCIQMC by minimizing the number of orbitals in the calculation. We find that, without embedding, *i*-FCIQMC struggles to converge these calculations due to their substantial system sizes and a lack of error cancellation between reactants and products. With embedding, the *i*-FCIQMC calculation converges straightforwardly to CCSD(T) benchmarks. Our results suggest that embedded *i*-FCIQMC will be able to treat system sizes well beyond our current reach (even though embedding introduces an error). We discuss how embedding might be improved (and thus the introduced error reduced) using *i*-FCIQMC energies as benchmarks.

I. INTRODUCTION

Catalysis often involves bond rearrangements at surfaces, a process featuring closely-separated energy minima, stretched bonds, and transition states. The electronic structure of these systems can become extremely complex; combined with energy differences that can be sub-millihartree, systematic study of catalytic bond rearrangements necessitates the development of new high-accuracy quantum chemistry methods. Although this is a subject of active and ongoing investigation, the high cost of wavefunction methods in particular prevents their widespread application.

One such method is full configuration interaction quantum Monte Carlo (FCIQMC) and its initiator adaptation (*i*-FCIQMC), which are part of a family of particularly attractive high-accuracy electronic structure methods that seek to combine the exactness of full configuration interaction (FCI) with the speed-ups achieved by quantum Monte Carlo (QMC).^{1,2} The first FCIQMC paper showed that the FCI ground-state wavefunction could be stochastically sampled due to the sparsity in the Hamiltonian;¹ it had previously been considered that there was no way to sample such a large vector as the exact FCI wavefunction. Since this pioneering work, many adaptations to FCIQMC and *i*-FCIQMC for calculating correlation energies of a wide variety of benchmark systems have been developed successfully.

i-FCIQMC has already been used for a variety of applications on relatively small systems, including model systems (such as the Hubbard model^{3,4} and the uniform electron gas^{5,6}) and dimers (such as C₂⁷ and Cr₂⁸). It has also seen more ambitious yet realistic applications, like iron porphyrins, which used a complete active space adaptation,⁹ and fully periodic nickel oxide chains¹⁰. A significant amount of investigation has also been aimed at using FCIQMC (and *i*-FCIQMC) to stochastically sample reduced density matrices within the FCIQMC method.^{11–16} Altogether, FCIQMC and its adaptations seem well-poised for answering important questions about the electronic structures of complex chemical systems.

Unfortunately, like all of its high-accuracy sister methods, *i*-FCIQMC is limited in its scope by its high cost: it can only treat relatively small system sizes (which here means number of electrons). Many further adaptations to *i*-FCIQMC have been developed to allow for the application of *i*-FCIQMC to larger systems. These adaptations include a combination of complete active space self-consistent field (CASSCF) with *i*-FCIQMC⁹, the semistochastic projector Monte Carlo method¹⁷, model space QMC,^{18,19} heat-bath configuration interaction,²⁰ perturbation theory²¹, stochastic multi-configurational self-consistent field theory (MCSCF) utilizing the FCIQMC methodology¹⁴, use of a transcorrelated Hamiltonian with *i*-FCIQMC^{22,23}, and combinations of the above methods, such as semistochastic heat-bath CI^{24–27}.

These efforts are made all the more relevant because there are also varieties of FCIQMC which broaden its applicability. Density matrix QMC,²⁸ has been developed

^{a)}These authors contributed equally to this paper

^{b)}Electronic mail: james-shepherd@uiowa.edu

for temperature-dependent electronic structure. Additionally, several FCIQMC methods have been developed for use on excited states, such as changing the underlying propagator²⁹, the Krylov-projected QMC method³⁰, utilizing a Löwdin partitioning technique¹⁸, using a Gram-Schmidt procedure³¹, and by restricting the population to the orthogonal complement of the low lying states³². The stochastic approach in the Slater determinant space has also been studied on the coupled cluster equations, called coupled cluster Monte Carlo.^{33–36} FCIQMC has also been adapted to treat the Clock Hamiltonian, to simulate the full time evolution of a quantum system.³⁷ Finally, some authors have developed a deterministic version of FCIQMC.³⁸ Others have developed a fast randomized iteration framework to essentially perform FCIQMC without walkers.³⁹

Quantum embedding methods were specifically developed to reduce the problem of scaling present in high level-methods such as *i*-FCIQMC. Embedding methods limit high-level calculations to a small subsystem that is embedded in the potential arising from the rest of the system, reducing the overall computational cost. When highly accurate embedding potentials are used, good accuracy can be achieved even when a subsystem is limited to a few atoms; therefore, embedding methodologies have been successfully applied to a wide variety of systems.^{40–54} Additionally, a large amount of work has been performed developing accurate embedding frameworks including quantum mechanics / molecular mechanics (QM/MM),⁵⁵ ONIOM,⁵⁶ density matrix embedding theory (DMET),⁵⁷ Green’s function embedding,^{58,59} and density functional theory (DFT) embedding.^{60–66} Many wavefunction methods such as CCSD(T), MP2, and CASPT2 have been embedded as the high-level theory; this work presents the first use of *i*-FCIQMC embedding.

The quantum embedding for this work was done using projection-based embedding,⁶⁷ which is DFT embedding method. Projection-based embedding is one solution to the non-additive kinetic energy problem of DFT embedding.^{68,69} The initial projection operator applied to this problem was the μ projection operator developed by the Manby and Miller groups.⁶⁷ This projection operator allows two embedded DFT subsystems (DFT-in-DFT) to exactly recreate full-system Kohn-Sham DFT. However, when embedding a wavefunction (WF) subsystem within a DFT environment (WF-in-DFT), the number of orbitals in the WF subsystem is the same as the number of orbitals in the full system. Since WF methods scale poorly with number of orbitals, basis set truncation methods were developed to reduce computational cost.^{70,71} The more recent truncation method removes basis functions from a subsystem when the density of that subsystem is below a threshold—a manner that maintains a high degree of accuracy. By decoupling the WF calculation from the total size of the system, WF-level energies may be calculated for systems consisting of hundreds of atoms. The μ operator method has shown a

high degree of accuracy for transition-metal and enzyme catalysis, and oxidation potentials of molecules in solution, among other systems of interest.^{69,72} Additionally, several groups have used the μ projection operator to embed multireference wavefunction methods for application to transition metal catalysts.^{73,74} These systems are inherently multireference; however, as the multireference character is localized to the metal center, μ embedding calculations were able to closely recreate experimental results.

Kállay and co-workers introduced the Huzinaga projection operator for DFT embedding;⁷⁵ however, that work truncated the orbitals by using local correlation methods. We showed that the Huzinaga projection operator could be used for aggressive truncation of the orbital space, where the densities could be absolutely localized on the atomic basis functions centered on atoms within the subsystem.⁷⁶ This allows for high computational efficiency as the WF subsystem has a greatly reduced number of molecular orbitals. Huzinaga projection embedding has also been successfully extended to periodic systems,⁷⁷ allowing for cluster or periodic WF calculations embedded in a periodic DFT environment. Given that the absolutely localized basis used in Huzinaga projection-based embedding reduces the number of orbitals to only those centered on the atoms of interest, we here determine the effectiveness of *i*-FCIQMC on an absolutely localized subsystem within the embedding potential of the full system.

We are generally motivated to increase the range and scope of systems available for study with *i*-FCIQMC. With a view toward our long-term interests in the study of bond-breaking and bond rearrangement on surfaces relevant to heterogeneous catalysis, we here study bond dissociation for diatomic molecules containing ionic or covalent bonds (specifically, LiH and HF, respectively) physisorbed onto a benzene molecule using *i*-FCIQMC. This type of calculation (with ~ 35 active electrons) is currently at the edge of applicability for *i*-FCIQMC; sometimes the system can be treated, and other times it cannot be treated. We show that embedding greatly alleviates the cost scaling of our model system. Specifically, data show that *i*-FCIQMC calculations performed on the full system (including both the diatomic molecule and the benzene molecule) fails to converge, whereas the system in which the benzene is represented by embedding converges with the same efficiency as an isolated molecular calculation. We analyze the type of convergence behaviors in *i*-FCIQMC and relate them to the differing electronic structures of the dissociation reactants and products. An important open question is the error due to embedding. We do not make an attempt to quantify this error because the full non-embedded system does not converge.

II. METHODS

A. i -FCIQMC

Full configuration interaction quantum Monte Carlo¹ and its initiator adaptation² attempt to solve for the ground-state wavefunction $|\Psi_0\rangle$ of the imaginary-time Schrödinger equation of a given Hamiltonian \hat{H} :

$$\frac{d|\Psi_0\rangle}{d\tau} = -\hat{H}|\Psi_0\rangle \quad (1)$$

where τ represents imaginary time. Beginning with a wavefunction that has non-zero overlap with the ground state, this equation can be solved in the long-imaginary-time limit to give the ground state wavefunction:

$$\lim_{\tau \rightarrow \infty} e^{-(\tau\hat{H}-S)}|D_0\rangle \propto |\Psi_0\rangle \quad (2)$$

where $|D_0\rangle$ is the reference Slater determinant, here taken to be the Hartree–Fock wavefunction. This relationship holds for any constant energy shift S . When long enough imaginary time τ has passed, S can be averaged, and the correlation energy ($E_{\text{corr}} = E_{\text{total}} - E_{\text{HF}}$) found.

The full configuration interaction wavefunction is typically written as a sum of Slater determinants, $|D_i\rangle$,

$$|\Psi_0\rangle = \sum_i c_i |D_i\rangle \quad (3)$$

As such, the imaginary time evolution operator acts in a determinant space.

Substituting Eq. (3) into Eq. (1) gives an expression which can be written as a finite difference

$$c_i^{m+1} - c_i^m = c_i^m \tau (-H_{ii} + S) - \sum_{j \neq i} c_j^m \tau H_{ij}. \quad (4)$$

Here, c_i^m is the coefficient of the i^{th} determinant at the m^{th} iteration of the simulation (after which $m\tau$ units of imaginary time have elapsed). The Hamiltonian is represented in the Slater determinant basis as:

$$H_{ij} = \langle D_i | \hat{H} | D_j \rangle \quad (5)$$

where δ_{ij} is the Kronecker delta. In the original FCIQMC algorithm, the weight c_i takes integer values.¹ The walker population N_w is given by $N_w = \sum_i c_i$. When S is varied to keep the walker population constant, its average becomes an estimate of the total ground-state energy.

The population of particles evolves towards the ground state using the following three steps introduced by Booth et al:

1. The particles with weight c_i are allowed to spawn from site i to a connected site j , where $H_{ij} \neq 0$ and $i \neq j$. The probability of spawning, $p(j|i)$ is uniform over the j which are connected by one or two electron excitations to i . The integer part of

$\frac{H_{ij}\tau}{p(j|i)}$ (including its sign) is then added to the weight at j . The non-integer remainder r is added with probability $|r|$ as ± 1 , where the sign comes from the sign of r .

2. Each particle with weight c_i changes its weight by $|S - H_{ii}|\tau$. As above, the integer part of $|S - H_{ii}|\tau$ is added to the weight at i . The non-integer remainder r treated as above.
3. Pairs of particles on the same site with opposite weight c_i annihilate each other and are removed from the simulation, leaving a population containing only a single sign on each site.

FCIQMC is not restricted to using only integer weights c_i . Real weights can be used; this adds a step to the above algorithm where the real weight is rounded off stochastically below a certain threshold (here, 0.01), chosen to reduce stochastic error and raise efficiency¹⁷.

The initiator adaption to FCIQMC, i -FCIQMC, separates the Slater determinant space to those with n_{add} (here, 3) or more walkers and those with fewer. If the origin of a spawning event (item 1. in the list above) is not an “initiator” and the spawning is attempted onto a site without walkers, H_{ij} is zeroed. The result is a dynamically-modified Hamiltonian, which profoundly influences convergence of the simulation. A simulation is only converged in the limit when changing the walker population no longer changes the energy (i.e., $N_w \rightarrow \infty$).

In practice, all i -FCIQMC needs to run is a correctly formatted integral table containing eigenvalues or orbital energies and electron repulsion integrals. These are used to compute Hamiltonian matrix elements using the Slater–Condon rules. The eigenvalues, ϵ_i , are the single-particle Hartree–Fock eigenvalue of the i^{th} orbital. All other integrals, v_{ijkl} , are electron repulsion integrals. We used pyscf as a source of integrals,⁷⁸ and the HANDE-QMC package to run i -FCIQMC.⁷⁹

A practical limitation that must be contended with when running an i -FCIQMC calculation is that the wavefunction must be sampled with sufficient detail in order to attain statistical and systematic convergence. As $N_w \rightarrow \infty$, the full configuration interaction (i.e. exact) limit is achieved; away from this limit, the calculation contains a small error termed the initiator error. This error typically converges as $\sim \exp(-\alpha N_w)$ and is challenging to extrapolate away. Reducing this error is crucial to the success of i -FCIQMC; its pre-factor/rate of decay is highly system dependent, and for larger systems can bottleneck the calculations.

B. Embedding

To perform i -FCIQMC-in-DFT embedding, the full system density is first split into two subsystems, subsystem A and subsystem B

$$\gamma^{\text{tot}} = \gamma^{\text{A}} + \gamma^{\text{B}} \quad (6)$$

where γ^A and γ^B are the densities matrices of subsystems A and B, respectively. We then obtain the DFT densities of the subsystems through a freeze-and-thaw algorithm.⁷⁶ This algorithm works by iteratively relaxing the density of subsystem A within the embedding potential and projection operator generated by the frozen density of subsystem B, and then freezing the subsystem A density and relaxing the subsystem B density within the embedding potential and projection operator generated by subsystem A until both subsystem densities have converged. The Fock matrix of subsystem A embedded in subsystem B can be written as

$$\mathbf{F}^{\text{A-in-B}} = \mathbf{h}^{\text{A-in-B}}[\gamma^A, \gamma^B] + \mathbf{g}[\gamma^A] \quad (7)$$

where \mathbf{g} contains the Coulomb and exchange-correlation potential for DFT—and the embedded core Hamiltonian is

$$\mathbf{h}^{\text{A-in-B}}[\gamma^A, \gamma^B] = \mathbf{h} + \mathbf{g}[\gamma^A + \gamma^B] - \mathbf{g}[\gamma^A] + \mathbf{P}^B \quad (8)$$

where \mathbf{h} is the one electron Hamiltonian, thus contains the kinetic and nuclear potential operators for both subsystems, and \mathbf{P}^B is the Huzinaga projection operator for subsystem A is given by

$$\mathbf{P}^B = -\frac{1}{2} \left(\mathbf{F}^{\text{AB}} \gamma^B \mathbf{S}^{\text{BA}} + \mathbf{S}^{\text{AB}} \gamma^B \mathbf{F}^{\text{BA}} \right), \quad (9)$$

where \mathbf{F}^{AB} and \mathbf{S}^{AB} are elements of the total Fock matrix and overlap matrix described over the basis functions of subsystems A and B. These equations are then analogously defined for the Fock matrix of B in A. Upon freeze-and-thaw convergence at the DFT level, the $\mathbf{h}^{\text{A-in-B}}[\gamma^A, \gamma^B]$ is used as the one-electron Hamiltonian for the *i*-FCIQMC calculation; thus, embedding only influences the one-electron integrals for the *i*-FCIQMC calculation. The final embedding energy is then

$$E_{\text{total}} = E_{\text{KS-DFT}}^{\text{total}} - E_{\text{DFT-in-DFT}}^{\text{A}} + E_{\text{iFCIQMC-in-DFT}}^{\text{A}}, \quad (10)$$

where $E_{\text{KS-DFT}}^{\text{total}}$ is the full-system Kohn-Sham (KS)-DFT energy, $E_{\text{DFT-in-DFT}}^{\text{A}}$ is the DFT energy of subsystem A embedded in the DFT potential of the rest of the system, and $E_{\text{iFCIQMC-in-DFT}}^{\text{A}}$ is the *i*-FCIQMC energy of subsystem A embedded in the DFT potential of the rest of the system.

C. Calculation details

The atomic coordinates of the systems under investigation were generated using the dispersion-corrected M06-D3 functional and the aug-cc-pVTZ basis set as implemented in Gaussian16. Six frozen orbitals were used for the $\text{C}_6\text{H}_6\text{-LiH}$ systems, and seven frozen orbitals were used for the $\text{C}_6\text{H}_6\text{-HF}$ system.

In our implementation, QSoME was modified to run integral calculations with pyscf.⁷⁸ The integrals were then

read in to the HANDE software package,⁷⁹ where they were used to perform *i*-FCIQMC calculations.

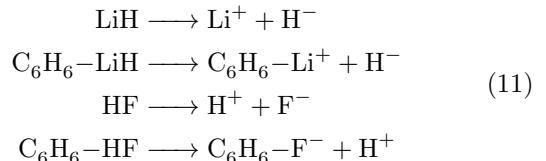
The *i*-FCIQMC calculations were performed using the open-source code HANDE-QMC. For the $\text{C}_6\text{H}_6\text{-LiH}$ system, an imaginary time step of 2×10^{-6} a.u. was used with 200,000 reports and 20 Monte Carlo cycles between reports. For the $\text{C}_6\text{H}_6\text{-HF}$ and $\text{C}_6\text{H}_6\text{-F}^-$ systems, a smaller time step of 9×10^{-7} a.u. was used due to the additional electrons present, with 400,000 reports for the first three target populations and 600,000 reports for the largest three target populations. A larger time step of 0.002 a.u. was used for the isolated LiH, HF and the embedded systems. In order to converge the calculations with respect to the target population, a range of target populations between 10^1 and 10^6 was used to generate the initiator curves.

Without the embedding algorithm, the LiH physisorbed on benzene system contains 34 electrons, requires 2.8×10^{41} determinants, and has a storage cost of 700 MB. After embedding is introduced, the subsystem treated with *i*-FCIQMC is reduced to 4 electrons and 2.9×10^4 determinants, with an integral storage cost of 440 KB.

III. RESULTS AND DISCUSSION

It is common for energy *differences* to yield better convergence (with respect to excitation rank, for example, in coupled cluster theory) than total energies themselves; this phenomenon, known as error cancellation, is a common benefit of running quantum-chemical calculations. In *i*-FCIQMC (in common with FCIQMC), a walker population of a given size (N_w) represents the wavefunction. The calculation is only exact if it is converged with respect to this walker number. An under-explored issue of *i*-FCIQMC calculations is that convergence is not faster for energy differences than for individual energies. The dissociation energies of LiH on benzene and HF on benzene represent two paradigmatic examples of how dissociation energies can be extremely challenging and costly to converge in *i*-FCIQMC due to a lack of error cancellation between reactants and products.

We hypothesize that adding benzene to straightforward LiH and HF dissociation energy calculations will cause *i*-FCIQMC to fail in a way that can be remedied by using embedding. To test our hypothesis, we calculate the energy changes associated with four reactions:



In particular, we reason that the dissociation energy of a LiH molecule physisorbed to benzene will be significantly more difficult to calculate using *i*-FCIQMC due to non-monotonic energy convergence with system size N . In

contrast with other methods, i -FCIQMC does not show error cancellation between systems that contain different numbers of electrons.

Figure 1 shows data we collected in support of our claim. Each of these plots is an initiator convergence plot, where the walker population is varied from 10^1 to 10^6 , and the energy is computed using i -FCIQMC. We plot the i -FCIQMC energy differences between reactants and products for the LiH and HF dissociation reactions, and compare these differences to CCSD(T) dissociation energies. CCSD(T) can serve as a good benchmark for initiator convergence: initiator error can vary greatly over many orders of magnitude in energy, and CCSD(T) is generally thought to have systematic error only on the order of 1 millihartree.

Figure 1(a) shows that isolated LiH and HF dissociation energies rapidly converge as a function of walker number, showing complete convergence at 10^4 and 10^5 walkers, respectively. The i -FCIQMC and CCSD(T) results are in agreement with each other to within 1 millihartree for $N_w \geq 10^3$, and within 10 millihartree for the smaller target populations. The HF dissociation converges in an oscillatory manner, because HF is slightly slower to converge than F^- ; in general, fine-grained oscillatory convergence has been shown in individual calculations.⁵ The HF system contains more variability at lower walker numbers than the LiH system, as is expected due to the higher number of electrons present in HF. As we expect, our results show that the isolated systems with small numbers of electrons converge with only modest convergence errors.

In contrast to the isolated molecules, convergence is difficult for the dissociation of molecules physisorbed on benzene. The convergence difficulties for these systems are shown in Fig. 1(b). The oscillatory behavior observed in Fig. 1(a) is magnified; in the case of HF, we are not able to converge this calculation at all in order to obtain a reaction energy, as the energy difference between 10^5 and 10^6 walkers is approximately -0.0597 hartree. Benzene adds 30 electrons to these systems; thus, significantly harder convergence is unsurprising. Again, since i -FCIQMC does not show error cancellation between systems containing different numbers of electrons, C_6H_6 -HF and C_6H_6 - F^- converge at different rates, which causes the energy difference between these two systems to be oscillatory. This is a key result of this manuscript that we explore later in further detail.

In Fig. 1(c), we present the results of the i -FCIQMC-in-DFT embedded systems. Since embedding decreases the number of electrons treated directly by i -FCIQMC, we are able to converge the i -FCIQMC energies of C_6H_6 -LiH and C_6H_6 -HF as easily as isolated LiH and HF. We see similar oscillatory behavior in the embedded calculations as we do for the isolated systems: Target populations 10^1 and 10^2 are still not very accurate. Fortunately, as we increase the target population, we see clear convergence. Comparing the three initiator curves across Fig. 1 reveals a similar convergence trend; this is

a very encouraging result, as it shows the i -FCIQMC-in-DFT embedding gives convergent results while simultaneously reducing the cost of these calculations significantly.

As computational cost is proportional to walker number, the ability to converge a calculation at 10^3 walkers compared with leaving it unconverged at 10^6 walkers represents a cost savings of at least 1000x. Data we present in the SI additionally show a 1000x savings in memory.

We fully appreciate that there is an unquantified embedding error in these calculations. This causes a change in ordering of the C_6H_6 -HF and C_6H_6 -LiH dissociation energies between Fig. 1(b) and Fig. 1(c) at the CCSD(T) level. For completeness, we note that the difference between CCSD(T) embedded calculations and full-system calculations give us an estimate of the i -FCIQMC embedding error as 0.45 millihartree and 4.80 millihartree for LiH and HF, respectively. However, our previous studies have shown that the embedding error can be further decreased by enlarging the wavefunction subsystem.⁷⁷ Although we are interested in quantifying the i -FCIQMC embedding error and using it to benchmark embedded CCSD(T), this analysis is beyond the scope of the proof-of-principle offered by this paper. One reason for this is that for a more realistic system, we would need to ask whether benzene or embedded benzene better represents the physical system. Another reason is that partitioning the system into two subsystems is also a source of error that is difficult to tease out from the embedding error.

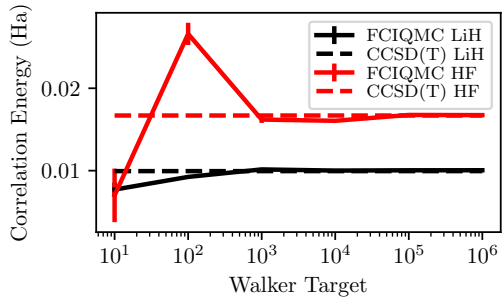
We now analyze the sources of error and the way that embedding overcomes convergence difficulties in i -FCIQMC.

A. Analysis of different convergence behaviors in i -FCIQMC

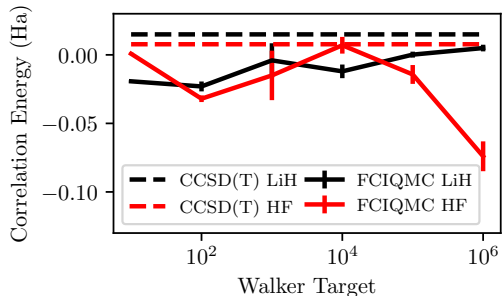
There are a number of analyses we can conduct in order to probe the extent of the non-convergent behavior described above in Fig. 1(b)—the case where all electrons in the benzene molecule are fully present in the i -FCIQMC calculation. In Fig. 2, the convergence of the reactants and products of dissociation for C_6H_6 -LiH and C_6H_6 -HF are shown. It can be seen from this figure that these calculations are not converged with respect to the number of walkers. This represents a particularly severe case where reactant and product energies actually cross over, which causes the energy differences to oscillate rather than converge smoothly, as observed in Fig. 1(b).

Both C_6H_6 -LiH and C_6H_6 -HF represent different types of challenges in convergence.

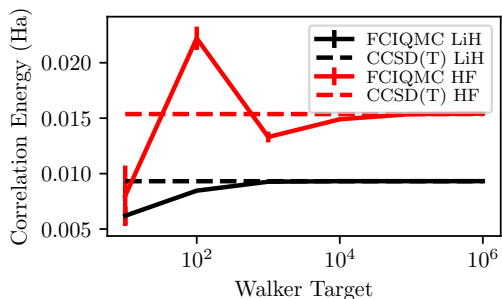
In C_6H_6 -HF, where reactants and products have the same number of electrons, each i -FCIQMC calculation appears to be smoothly converging as a function of walker number. Prior work has established the appearance of such smooth convergence as a stretched exponential in the walker population, $\exp(-N_w^\alpha)$, $\alpha \ll 1.0$.⁷ The decay



(a)



(b)



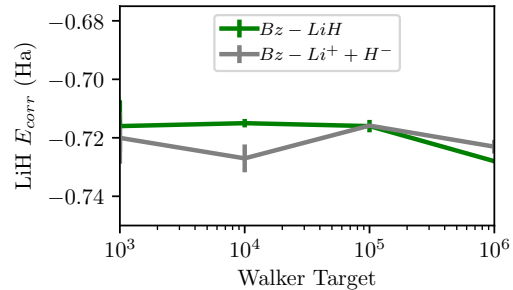
(c)

Figure 1. Correlation energy contribution to the dissociation energies of cc-pVDZ LiH and HF for molecules that are (a) isolated (4 and 10 electrons respectively), (b) physisorbed to benzene (34 and 40 electrons respectively), (c) physisorbed to benzene and embedded (4 and 10 electrons treated explicitly with i -FCIQMC). The i -FCIQMC calculations, shown as solid lines, were performed with six target populations ranging from 10^1 to 10^6 on a logarithmic scale. Good agreement is achieved between i -FCIQMC and CCSD(T) for isolated and embedded systems.

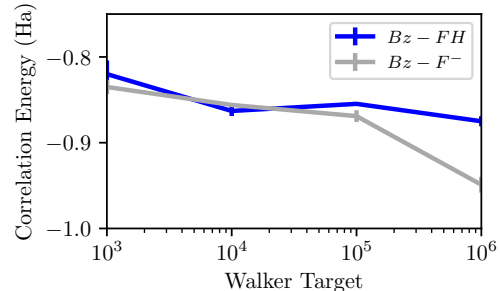
parameters are highly system-dependent; as such, two converging calculations could easily cross over one another. The general form of two converging calculations is:

$$E_{\text{corr,A-B}} = E_{\text{corr,A}} - E_{\text{corr,B}} + A_1 e^{-N_w^{\alpha_1}} - A_2 e^{-N_w^{\alpha_2}} \quad (12)$$

In the case of HF, the combined initiator error, $A_1 e^{-N_w^{\alpha_1}} - A_2 e^{-N_w^{\alpha_2}}$, obscures or is much larger than the term $E_{\text{corr,A}} - E_{\text{corr,B}}$. As a result, the reaction en-



(a)



(b)

Figure 2. The initiator curves at walker numbers $N_w = 10^3$ through 10^6 for the products and reactants of the dissociation reactions of (a) LiH and (b) HF physisorbed on benzene.

ergy fails to converge, instead oscillating even at large walker numbers.

The underlying reason for the differences in convergence between $\text{C}_6\text{H}_6\text{-HF}$ and $\text{C}_6\text{H}_6\text{-F}^-$ is not known. It seems likely that the form of the stretched exponential is itself related to excited state decays in imaginary time, although this has not been established in the literature. Specifically, the overlap between the simulation wavefunction in imaginary time, $|\Psi(\tau)\rangle$, and the FCI excited states, $|\Psi_i\rangle$, is expected to decay exponentially in imaginary time:⁷

$$\langle \Psi(\tau) | \Psi_i \rangle = C_i \exp(-\tau(E_i - E_0)) \quad (13)$$

where E_i and E_0 are the excited state and ground state energy eigenvalues, respectively. In this picture, then, a simulation with insufficient walker population would have to get stuck somewhere between one state and another in a way that cannot be resolved by projecting out over more imaginary time steps, because there is not enough information in each timestep to afford resolution of the ground state.

The case of $\text{C}_6\text{H}_6\text{-LiH}$ is a little different, since $\text{C}_6\text{H}_6\text{-Li}^+$ exhibits oscillatory convergence already. This case of oscillatory fine structure has been seen before, such as in studies of the uniform electron gas.⁵ This on its own hampers convergence, lending an oscillatory character to the reaction energy independent of whether these calculations are themselves converging to the correct energy.

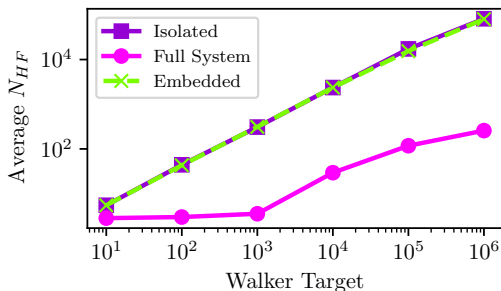


Figure 3. The population of walkers on the Hartree–Fock determinant in the i -FCIQMC calculation with respect to iteration for each target population of $N_w = 10^1$ to 10^6 for each of three LiH systems: isolated LiH, the full system C_6H_6 -LiH and the embedded C_6H_6 -LiH.

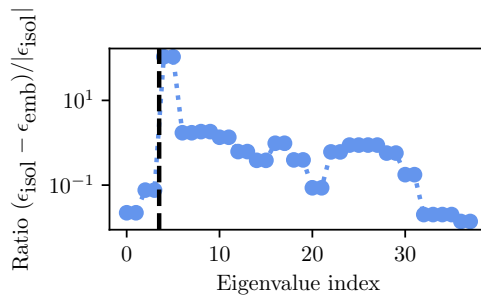
B. Hartree–Fock Population

Another measure by which we can compare the isolated and embedded calculations is the number of walkers present on the Hartree–Fock determinant (shown in Fig. 3). This population is sometimes used as a means to determine convergence of an i -FCIQMC calculation, since, in the early phase of an i -FCIQMC calculation, it does not vary from its baseline of $[O(1)]$ walker. The number of walkers on the Hartree–Fock determinant also confirms the different convergence behaviors of the full, isolated, and embedded systems: The embedded and isolated systems have Hartree–Fock populations that grow at the same rate, whereas the full system has many fewer of these kind of walkers. In terms of the walker dynamics, the larger number of determinants in the full system depletes the signal present on the Hartree–Fock determinant and slows convergence.

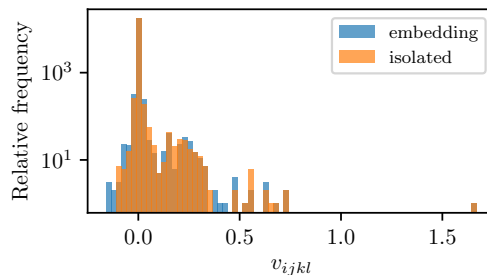
C. Embedding and the sign problem in i -FCIQMC

The sign problem in FCIQMC has been related to the amount of spin frustration in the system: each Slater determinant in the system needs to find its sign over the course of a simulation.⁴ Specifically, the eigenvalue of a matrix $H'_{ij} = \delta_{ij}H_{ij} - (1 - \delta_{ij})|H_{ij}|$ whose eigenstate has entirely non-negative components and contaminates solutions.

The signs in H come from the four-index integrals via the Slater–Condon rules, and so it is important to discuss whether there is a significant change in the integrals due to embedding. In Fig. 4, we show a comparison of two types of integrals that are passed between the embedding code and i -FCIQMC for isolated C_6H_6 -LiH compared with embedded C_6H_6 -LiH. In this case, the LiH eigenvalues are generally lowered by between -0.01 hartree to -0.3 hartree by embedding. The specific ratio for each eigenvalue is plotted against its energy-ordered index in Fig. 4(a), showing that as the eigenvalue becomes higher in energy, it is also affected less by embedding. We show the effect on the electron repulsion integrals in Fig. 4(b),



(a)



(b)

Figure 4. Changes in the LiH integral table for i -FCIQMC represented through (a) differences between eigenvalues ϵ_i for the embedding and isolated systems, where the black dashed line represents the division between occupied and virtual Hartree–Fock orbitals, and (b) electron repulsion integrals v_{ijkl} for both embedded and isolated systems.

where the distribution of the ~ 1800 integrals is presented as a histogram. The molecular orbitals differ between the isolated case and the embedding case and this leads to the small changes in the electron repulsion integrals. From the plots above, we would expect that there is not an increase in the complexity of the sign problem, since most matrix elements remain unchanged.

IV. CONCLUSIONS

In summary, we here examined convergence difficulties present when using i -FCIQMC to calculate the electronic structure of large systems by exploring the bond dissociations of two prototypical molecules, LiH and HF, physisorbed to benzene. Since i -FCIQMC does not show error cancellation between systems with different numbers of electrons, the energy differences between reactants and products tended to oscillate. As a result, dissociation energies calculated from i -FCIQMC did not converge. To remedy the convergence issues that i -FCIQMC has with large systems, we embedded i -FCIQMC in DFT. We showed that this new embedded i -FCIQMC was better able to converge dissociation energies, giving results that agree with our CCSD(T) benchmarks. This agreement demonstrates the robust-

ness of the absolute localization approach for Huzinaga projection-based embedding and the ability to use high-level i -FCIQMC wavefunctions embedded in DFT.

Since embedded i -FCIQMC also reduces the number of electrons (and thus orbitals) in a calculation, embedded i -FCIQMC calculations run with substantially lower cost than full i -FCIQMC, alleviating the method's reduced-exponential cost scaling. Based on our results, we estimate the cost saving to be at least 1000x in compute time and 1000x in memory for the model systems studied here. Whereas for larger systems, i -FCIQMC calculations can be computationally intractable while embedded i -FCIQMC calculations will remain feasible. There are applications for which CCSD(T) fails to give good answers, such as those involving strong correlation or bond breaking; i -FCIQMC can treat these applications with high accuracy. As such, we believe that i -FCIQMC embedded in DFT is a significant and realistic step forward for bringing i -FCIQMC towards the routine treatment of real applications, as DFT embedding both alleviates convergence concerns and dramatically reduces the cost of the method.

One limitation of this work is that we have not analyzed the added error in the correlation energy introduced when undertaking embedding, since we believe it is outside of the scope of a proof-of-principle and deserves much more attention on its own. Since CCSD(T) can treat the full systems for the prototypical bond dissociations studied in this manuscript, we *could* have added a correction to our embedded i -FCIQMC arising from the CCSD(T) energy difference between the full and embedded systems; this may be a way forward for future work. We could also treat a system that is small enough to examine the full system with i -FCIQMC, resulting in our being able to benchmark the embedding error for the benefit of other practitioners. In reality, there are also applications where a course-grained model of the environment is the best that we can do at any level of theory, because some inaccuracy comes from not knowing the positions and identities of the atoms involved. Such situations include solvated ions, surface reconstruction, and transition states.

The technical achievement of this manuscript is the combination of mean-field solver codes (QSoME/pyscf) with that of the i -FCIQMC code (HANDE). We also wish to highlight that the technical achievement presented here was only possible because all of the codes used were open source, allowing us to quickly and accurately interface calculations from disparate quantum chemistry implementations. The value of open-source computing has been highlighted by one of us (JS) elsewhere.⁸⁰

In closing, we believe that this study highlights an important step forward for both i -FCIQMC and embedding. We believe that the work presented here brings the community one step closer to the routine application of high-accuracy electronic structure to study strongly-correlated systems of chemical and technological interest.

V. ACKNOWLEDGEMENTS

This research is supported by the Nanoporous Materials Genome Center, funded by the U.S. Department of Energy, Office of Basic Energy Sciences, Division of Chemical Sciences, Geosciences and Biosciences under Award DE-FG02-17ER16362. DG and JG acknowledge an award of computer time was provided by the ASCR Leadership Computing Challenge (ALCC) program. This research used resources of the National Energy Research Scientific Computing Center (NERSC), a U.S. Department of Energy Office of Science User Facility operated under Contract No. DE-AC02-05CH11231. DG and JG acknowledge additional computer resources were provided by the Minnesota Supercomputing Institute (MSI) at the University of Minnesota. JJS and HRP acknowledge the University of Iowa for funding and the University of Iowa Informatics Initiative (UI3) for computer resources. The code used throughout this work was HANDE (hande.org.uk), QSoME (github.com/Goodpaster/QSoME), and pySCF (sunqm.github.io/pyscf/).

REFERENCES

- G. H. Booth, A. J. W. Thom, and A. Alavi, *J. Chem. Phys.* **131**, 054106 (2009).
- D. Cleland, *The initiator Full Configuration Interaction Quantum Monte Carlo method: Development and applications to molecular systems*, Ph.D. thesis, University of Cambridge (2009).
- L. R. Schwarz, G. H. Booth, and A. Alavi, *Phys. Rev. B* **91**, 045139 (2015).
- J. S. Spencer, N. S. Blunt, and W. M. C. Foulkes, *J. Chem. Phys.* **136**, 054110 (2012).
- J. J. Shepherd, G. H. Booth, and A. Alavi, *J. Chem. Phys.* **136**, 244101 (2012).
- J. J. Shepherd, G. Booth, A. Grüneis, and A. Alavi, *Phys. Rev. B* **85**, 081103 (2012).
- G. H. Booth, D. Cleland, A. J. W. Thom, and A. Alavi, *J. Chem. Phys.* **135**, 084104 (2011).
- G. H. Booth, S. D. Smart, and A. Alavi, *Mol. Phys.* **0**, 1 (2014).
- G. Li Manni, S. D. Smart, and A. Alavi, *J. Chem. Theory Comput.* **12**, 1245 (2016).
- G. H. Booth, A. Grüneis, G. Kresse, and A. Alavi, *Nature* **493**, 365 (2013).
- C. Overy, G. H. Booth, N. S. Blunt, J. J. Shepherd, D. Cleland, and A. Alavi, *J. Chem. Phys.* **141**, 244117 (2014).
- G. H. Booth, D. Cleland, A. Alavi, and D. P. Tew, *J. Chem. Phys.* **137**, 164112 (2012).
- R. E. Thomas, D. Opalka, C. Overy, P. J. Knowles, A. Alavi, and G. H. Booth, *J. Chem. Phys.* **143**, 054108 (2015).
- R. E. Thomas, Q. Sun, A. Alavi, and G. H. Booth, *J. Chem. Theory Comput.* **11**, 5316 (2015).
- N. S. Blunt, G. H. Booth, and A. Alavi, *J. Chem. Phys.* **146**, 244105 (2017).
- N. S. Blunt, S. D. Smart, J. A. F. Kersten, J. S. Spencer, G. H. Booth, and A. Alavi, *J. Chem. Phys.* **142**, 184107 (2015).
- F. R. Petruziello, A. A. Holmes, H. J. Changlani, M. P. Nightingale, and C. J. Umrigar, *Phys. Rev. Lett.* **109** (2012), 10.1103/PhysRevLett.109.230201.
- S. Ten-no, *J. Chem. Phys.* **138**, 164126 (2013).
- Y. Ohtsuka and S. Ten-no, *J. Chem. Phys.* **143**, 214107 (2015).
- A. A. Holmes, N. M. Tubman, and C. J. Umrigar, *J. Chem. Theory Comput.* **12**, 3674 (2016).

- ²¹N. S. Blunt, *J. Chem. Phys.* **148**, 221101 (2018).
- ²²S. Sharma, T. Yanai, G. H. Booth, C. J. Umrigar, and G. K.-L. Chan, *J. Chem. Phys.* **140**, 104112 (2014).
- ²³H. Luo and A. Alavi, *J. Chem. Theory Comput.* **14**, 1403 (2018).
- ²⁴S. Sharma, A. A. Holmes, G. Jeanmairet, A. Alavi, and C. J. Umrigar, *J. Chem. Theory Comput.* **13**, 1595 (2017).
- ²⁵A. A. Holmes, C. J. Umrigar, and S. Sharma, *J. Chem. Phys.* **147**, 164111 (2017).
- ²⁶J. Li, M. Otten, A. A. Holmes, S. Sharma, and C. J. Umrigar, *J. Chem. Phys.* **149**, 214110 (2018).
- ²⁷A. D. Chien, A. A. Holmes, M. Otten, C. J. Umrigar, S. Sharma, and P. M. Zimmerman, *The Journal of Physical Chemistry A* **122**, 2714 (2018).
- ²⁸N. S. Blunt, T. W. Rogers, J. S. Spencer, and W. M. C. Foulkes, *Phys. Rev. B* **89**, 245124 (2014).
- ²⁹G. H. Booth and G. K.-L. Chan, *J. Chem. Phys.* **137**, 191102 (2012).
- ³⁰N. Blunt, A. Alavi, and G. H. Booth, *Phys. Rev. Lett.* **115** (2015), 10.1103/PhysRevLett.115.050603.
- ³¹N. S. Blunt, S. D. Smart, G. H. Booth, and A. Alavi, *J. Chem. Phys.* **143**, 134117 (2015).
- ³²A. Humeniuk and R. Mitri, *J. Chem. Phys.* **141**, 194104 (2014).
- ³³A. J. W. Thom, *Phys. Rev. Lett.* **105** (2010), 10.1103/PhysRevLett.105.263004.
- ³⁴R. S. T. Franklin, J. S. Spencer, A. Zocante, and A. J. W. Thom, *J. Chem. Phys.* **144**, 044111 (2016).
- ³⁵J. E. Deustua, J. Shen, and P. Piecuch, *Phys. Rev. Lett.* **119** (2017), 10.1103/PhysRevLett.119.223003.
- ³⁶C. J. C. Scott and A. J. W. Thom, *J. Chem. Phys.* **147**, 124105 (2017).
- ³⁷J. R. McClean and A. Aspuru-Guzik, *Phys. Rev. A* **91** (2015), 10.1103/PhysRevA.91.012311.
- ³⁸N. M. Tubman, J. Lee, T. Y. Takeshita, M. Head-Gordon, and K. B. Whaley, *J. Chem. Phys.* **145**, 044112 (2016).
- ³⁹S. M. Greene, R. J. Webber, J. Weare, and T. C. Berkelbach, [arXiv:1905.00995 \[cond-mat, physics:physics\]](https://arxiv.org/abs/1905.00995) (2019), arXiv:1905.00995.
- ⁴⁰S. A. French, A. A. Sokol, S. T. Bromley, C. R. A. Catlow, S. C. Rogers, F. King, and P. Sherwood, *Angewandte Chemie International Edition* **40**, 4437 (2001).
- ⁴¹S. A. French, A. A. Sokol, S. T. Bromley, C. R. A. Catlow, S. C. Rogers, and P. Sherwood, *The Journal of Chemical Physics* **118**, 317 (2003).
- ⁴²L. W. Chung, W. M. C. Sameera, R. Ranzani, A. J. Page, M. Hatanaka, G. P. Petrova, T. V. Harris, X. Li, Z. Ke, F. Liu, H.-B. Li, L. Ding, and K. Morokuma, *Chemical Reviews* **115**, 5678 (2015).
- ⁴³T. Vreven and K. Morokuma, *Theoretical Chemistry Accounts: Theory, Computation, and Modeling (Theoretica Chimica Acta)* **109**, 125 (2003).
- ⁴⁴Y. JOSHI and K. THOMSON, *Journal of Catalysis* **230**, 440 (2005).
- ⁴⁵A. A. Sokol, S. T. Bromley, S. A. French, C. R. A. Catlow, and P. Sherwood, *International Journal of Quantum Chemistry* **99**, 695 (2004).
- ⁴⁶J. D. Goodpaster, T. A. Barnes, F. R. Manby, and T. F. Miller, *The Journal of Chemical Physics* **140**, 18A507 (2014), <https://doi.org/10.1063/1.4864040>.
- ⁴⁷P. Huo, C. Uyeda, J. D. Goodpaster, J. C. Peters, and T. F. Miller, *ACS Catalysis* **6**, 6114 (2016), <https://doi.org/10.1021/acscatal.6b01387>.
- ⁴⁸D. Claudino and N. J. Mayhall, *Journal of Chemical Theory and Computation* **15**, 1053 (2019), <https://doi.org/10.1021/acs.jctc.8b01112>.
- ⁴⁹F. Ding, T. Tsuchiya, F. R. Manby, and T. F. Miller, *Journal of Chemical Theory and Computation* **13**, 4216 (2017), pMID: 28783359, <https://doi.org/10.1021/acs.jctc.7b00666>.
- ⁵⁰F. Ding, F. R. Manby, and T. F. Miller, *Journal of Chemical Theory and Computation* **13**, 1605 (2017), pMID: 28245122, <https://doi.org/10.1021/acs.jctc.6b01065>.
- ⁵¹K. Miyamoto, T. F. Miller, and F. R. Manby, *Journal of Chemical Theory and Computation* **12**, 5811 (2016), pMID: 27749063, <https://doi.org/10.1021/acs.jctc.6b00685>.
- ⁵²M. E. Fornace, J. Lee, K. Miyamoto, F. R. Manby, and T. F. Miller, *Journal of Chemical Theory and Computation* **11**, 568 (2015), pMID: 26580914, <https://doi.org/10.1021/ct5011032>.
- ⁵³M. E. Fornace, J. Lee, K. Miyamoto, F. R. Manby, and T. F. Miller, *Journal of Chemical Theory and Computation* **11**, 3968 (2015), pMID: 26574476, <https://doi.org/10.1021/acs.jctc.5b00630>.
- ⁵⁴P. Ramos, M. Papadakis, and M. Pavanello, *The Journal of Physical Chemistry B* **119**, 7541 (2015), pMID: 25845645, <https://doi.org/10.1021/jp511275e>.
- ⁵⁵A. Warshel and M. Levitt, *Journal of Molecular Biology* **103**, 227 (1976).
- ⁵⁶M. Svensson, S. Humbel, R. D. J. Froese, T. Matsubara, S. Sieber, and K. Morokuma, *The Journal of Physical Chemistry* **100**, 19357 (1996).
- ⁵⁷G. Knizia and G. K.-L. Chan, *Journal of Chemical Theory and Computation* **9**, 1428 (2013).
- ⁵⁸G. Onida, L. Reining, and A. Rubio, *Reviews of Modern Physics* **74**, 601 (2002).
- ⁵⁹W. Chibani, X. Ren, M. Scheffler, and P. Rinke, *Physical Review B* **93**, 165106 (2016).
- ⁶⁰C. R. Jacob and J. Neugebauer, *Wiley Interdisciplinary Reviews: Computational Molecular Science* **4**, 325 (2014).
- ⁶¹T. A. Wesolowski and Y. A. Wang, *Recent Progress in Orbital-free Density Functional Theory*, Recent Advances in Computational Chemistry, Vol. 6 (WORLD SCIENTIFIC, 2013).
- ⁶²T. A. Wesolowski (2006) pp. 1–82.
- ⁶³J. Neugebauer, *Physics Reports* **489**, 1 (2010).
- ⁶⁴W. Yang, *Physical Review Letters* **66**, 1438 (1991).
- ⁶⁵C. Huang, M. Pavone, and E. A. Carter, *The Journal of Chemical Physics* **134**, 154110 (2011).
- ⁶⁶J. D. Goodpaster, N. Ananth, F. R. Manby, and T. F. Miller, *The Journal of Chemical Physics* **133**, 084103 (2010).
- ⁶⁷F. R. Manby, M. Stella, J. D. Goodpaster, T. F. Miller, and T. F. Miller III, *Journal of chemical theory and computation* **8**, 2564 (2012).
- ⁶⁸J. D. Goodpaster, T. A. Barnes, F. R. Manby, and T. F. Miller, *The Journal of Chemical Physics* **140**, 18A507 (2014).
- ⁶⁹S. J. R. Lee, M. Welborn, F. R. Manby, and T. F. Miller, *Cite This: Acc. Chem. Res* **52**, 1359 (2019).
- ⁷⁰T. A. Barnes, J. D. Goodpaster, F. R. Manby, and T. F. Miller, *J. Chem. Phys.* **139**, 24103 (2013).
- ⁷¹S. J. Bennie, M. Stella, T. F. Miller, and F. R. Manby, *The Journal of Chemical Physics* **143**, 024105 (2015).
- ⁷²J. D. Goodpaster, T. A. Barnes, F. R. Manby, and T. F. Miller, *J. Chem. Phys.* **137**, 224113 (2012).
- ⁷³A. Chapovetsky, M. Welborn, J. M. Luna, R. Haiges, T. F. Miller, and S. C. Marinescu, *ACS Central Science* **4**, 397 (2018).
- ⁷⁴A. P. de Lima Batista, A. G. S. de Oliveira-Filho, and S. E. Galembeck, *Physical Chemistry Chemical Physics* **19**, 13860 (2017).
- ⁷⁵B. Hgely, P. R. Nagy, G. G. Ferenczy, and M. Kllay, *The Journal of Chemical Physics* **145**, 064107 (2016), <https://doi.org/10.1063/1.4960177>.
- ⁷⁶D. V. Chulhai and J. D. Goodpaster, *Journal of Chemical Theory and Computation* **13**, 1503 (2017).
- ⁷⁷D. V. Chulhai and J. D. Goodpaster, *Journal of Chemical Theory and Computation* **14**, 1928 (2018).
- ⁷⁸
- ⁷⁹J. S. Spencer, N. S. Blunt, S. Choi, J. Etrych, M.-A. Filip, W. M. C. Foulkes, R. S. T. Franklin, W. J. Handley, F. D. Malone, V. A. Neufeld, R. Di Remigio, T. W. Rogers, C. J. C. Scott, J. J. Shepherd, W. A. Vigor, J. Weston, R. Xu, and A. J. W. Thom, *J. Chem. Theory Comput.* **15**, 1728 (2019).
- ⁸⁰J. S. Spencer, N. S. Blunt, W. A. Vigor, F. D. Malone, W. M. C. Foulkes, J. J. Shepherd, and A. J. W. Thom, *Journal of Open Research Software* **3** (2015), 10.5334/jors.bw.